Ain Shams Engineering Journal xxx (xxxx) xxx

Contents lists available at ScienceDirect

Ain Shams Engineering Journal

journal homepage: www.sciencedirect.com

Engineering of uniform anisotropic interconnection system with polyimide films for flexible electronics

Heebo Ha [a,1], Byunghoon Lee [b,1], Sooyong Choi [a], Nadeem Qaiser [c], Sera Kwon [b], Zungsun Choi [d], Chih-Ming Chen [e], Byungil Hwang [a,f,*]

[a] Department of Intelligent Semiconductor Engineering, Chung-Ang University, Seoul 06974, Republic of Korea
[b] Manufacturing Core Technology Team / Global Technology Research, Samsung Electronics, Suwon, Republic of Korea
[c] Electrical Engineering, Computer, Electrical and Mathematical Sciences, and Engineering Division, King Abdullah University of Science and Technology (KAUST), Thuwal, 23955-6900, Saudi Arabia
[d] School of Engineering, Handong Global University, Pohang, 37554, Republic of Korea
[e] Department of Chemical Engineering, National Chung Hsing University, Taichung 402202, Taiwan
[f] School of Integrative Engineering, Chung-Ang University, Seoul 06974, Republic of Korea

ARTICLE INFO

Keywords:
Anisotropic conductive film
Anisotropic interconnection system
Flexible electronics
Polyimide films

ABSTRACT

To address the drawbacks of conventional anisotropic conductive films in flexible electronics, this study explored a novel flexible interconnection system comprising a flexible polyimide (PI) film with uniformly distributed Cu-filled holes. Periodic holes were formed along the PI film thickness. The holes were filled with Cu via electroplating, and both sides of the Cu ends were electrolessly Sn-plated to form solder bumps. The resulting Sn-coated Cu vias exhibited low electrical resistance (22 mΩ) and high shear bonding strength (63.76 MPa). Nonconductive adhesive layers were applied on both sides of the films. Consequently, the interconnected chips exhibited a high shear bonding strength (85.55 MPa) and electrical conductivity (22 mΩ), maintaining 98.84 % and 100 % of the initial values respectively, even after 1,000 cycles of bending and ambient stability test at 85 ℃. Light-emitting diodes integrated with a flexible printed circuit board using the proposed system demonstrated uninterrupted brightness, even under bending.

1. Introduction

The emergence of flexible electronics and 5G wireless communication systems has spurred extensive research on applications that seek to enhance data processing speed and user convenience [1–8]. Innovations such as flexible displays, electronic skins, and medical devices have rapidly evolved in response to the growing demand for flexible interconnection systems [9–15]. Anisotropic conductive films (ACFs) have attracted considerable attention as a flexible interconnection method because of their mechanical flexibility and easy processability via simple hot pressing on polymer-based flexible substrates such as Flex-on-Glass and Flex-on-Board [16–20]. ACFs comprise insulating polymer matrices with embedded conductive particles. They are placed between the metal pads and electrodes of the integrated circuit (IC) substrates, which are then mechanically pressed with heat. Under heat pressing, only the conductive particles between the metal pads are highly pressed to form electrical contacts, thereby creating an electronic pathway between the metal pads of the electronic component and the electrodes of the substrates [20–23].

Despite these advantages, one of the key challenges associated with ACFs is unintended pathway formation or short circuits owing to the clustering of conductive particles or solder balls within the matrix [24–26]. Moreover, increased resistance at the interface between conductive particles, diminished bond strength over the lifespan of electronic devices, and particle displacement due to changes in temperature or vibration may result in open-circuit failures in the ICs [27]. Therefore, prior studies have sought to uniformly distribute the conductive particles in the matrix [28–30]. Park et al [31]. utilized a magnetic field to uniformly distribute conductive particles in an ACF. The Ni-coated particles were dispersed in polyvinylidene fluoride under a magnetic field along the thickness direction. By applying a magnetic field of 1600 G, 80 % of the particles were uniformly arranged along the

* Corresponding author at: Department of Intelligent Semiconductor Engineering, Chung-Ang University, Seoul 06974, Republic of Korea.
E-mail address: bihwang@cau.ac.kr (B. Hwang).
[1] These authors contributed equally to this work.

https://doi.org/10.1016/j.asej.2024.103064
Received 9 July 2024; Received in revised form 26 August 2024; Accepted 11 September 2024
2090-4479/© 2024 THE AUTHORS. Published by Elsevier BV on behalf of Faculty of Engineering, Ain Shams University. This is an open access article under the CC BY-NC-ND license (http://creativecommons.org/licenses/by-nc-nd/4.0/).

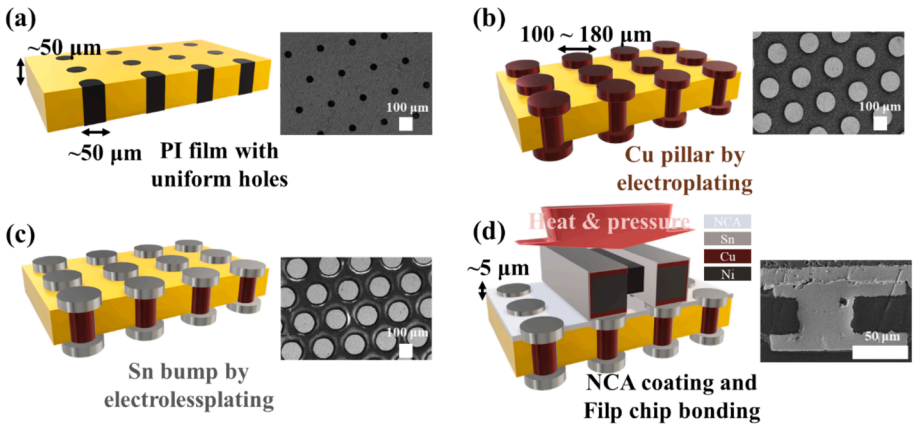


Fig. 1. (a–d) Schematics of fabrication process of the holey PI-based flexible interconnection system.

film thickness, thereby avoiding aggregation. Although the application of a magnetic field improved the uniformity of the dispersion of conductive particles in the ACF, the remaining 20 % of the particles remained nonuniformly dispersed. To further improve the uniformity, Hwang et al [28] proposed the creation of periodic holes in the polymer matrix and filling the holes with conductive particles. They made an octadecyl trichlorosilane-coated polydimethylsiloxane (PDMS) pillar stamp, which were pressed into PDMS substrates to render periodic holes with 20 μm diameter. Subsequently, Au-coated polystyrene (PS) microspheres were placed in the holes through mechanical rubbing, achieving 99 % distribution of the PS particles. The resulting ACF mitigated most of the problems resulting from the undesired agglomeration of particles. However, the contact between the Au-coated PS and metal pad was not sufficiently stable to realize reliability under deformable conditions. In an effort to enhance the electrical and mechanical properties of ACF under deformable conditions, Bo et al [32] demonstrated a liquid metal (LM)-based ACFs. Eutectic galinstan (EGaInSn)-based liquid metal particles were uniformly dispersed in epoxy resin by using a tip sonicator. Under mechanical press in a vertical direction by chips and substrates, the LM particles were collapsed that formed conductive paths with the sufficient adhesion strength and low electrical resistance of 0.6 O. However, the LM-based ACF have the risk of short circuit by the connection of LMs through in plane direction. Thus, the development of a new ACF system with perfectly distributed conductive paths that can achieve high mechanical stability and electrical conductivity is urgently needed.

This study entailed the development of a new flexible interconnection method by using a holey polyimide (PI) film, addressing the major drawbacks of conventional ACF. We created uniformly distributed Cu-filled holes in PI films. Both sides of the Cu were plated with Sn via electroless deposition to enhance its electrical conductivity and bonding strength with the metal electrodes. The synergistic integration of the highly conductive Cu, flexible PI, and reliable Sn solder bumps resulted in a novel ACF system that was mechanically stable under bending and electrically conductive, while exhibiting excellent bonding properties. In addition, we demonstrated the direct integration of our ACF system into mini-light-emitting diodes (LEDs) by utilizing a flexible printed circuit board.

2. Materials and methods

2.1. Material

Copper sulfate solution ($CuSO_4$; 98 %) was purchased from Hantech PMC. Stannous sulfate solution ($SnSO_4$, 95 %) was purchased from CNC Tech. The Ti etchant (GE-8148) was purchased from Transene Company, Inc. Test chips for bond strength (0.8 mm wide × 1.6 mm long × 0.5 mm thick) were purchased from Samsung Electronics. Mini-LEDs (0.8 mm wide × 1.6 mm long × 0.5 mm thick) were purchased from Nationstar Optoelectronics Co., Ltd. The PI film was washed with ethanol and deionized water prior to the experiment. PI films featuring an arranged array of through holes were custom-fabricated. The fabrication process entailed the formation of perforations using a femtosecond infrared (IR) laser through a direct writing process. Mechanical polishing was then performed on drilled PI to eliminate burrs.

2.2. Characterization

The deposited bumps and cross-sectional images were analyzed via scanning electron microscopy (SEM; S-3400 N, Hitachi) and energy-dispersive spectroscopy (EDS; NORAN System 7, Thermo). The shear strength was measured using chips comprising Cu and Sn layers attached to a PI film. The chips were bonded to PI films at a pressure of 1.2 MPa for 20 s in the range of 240–270 ℃. The test was conducted under the following conditions. The PI film was cut into 20 mm × 20 mm samples; the stretching speed was 100 μm/s; and a tip size of 2 mm was employed in the shear strength tester (Dage 4000, Nordson). Mechanical reliability tests were conducted using a cyclic bending tester (CK Materials, South Korea) under a bending radius of 1.5 mm for 1000 cycles. The details of the cyclic bending tester can be founded in ref. [33]. Further, the current (I)–voltage (V) curve was obtained using a DC current source (Keithley 6200, Tektronix), and the operation of the LED were checked by attaching LEDs in a 3 × 3 array, under the same conditions as the chip.

2.3. Sample preparation

The PI film with uniformly distributed holes had a thickness of approximately 50 μm, with hole diameters of around 50 μm and an average spacing of approximately 200 μm between the holes. A 50 nm thick Ti seed layer was deposited on one side of the PI film using direct current magnetron sputtering at 100 W for 12 min at room temperature. And Cu was electroplated at room temperature using a hull cell rectifier (Jungdo Test Instruments Lab) in a 1 L bath containing 600 mL of $CuSO_4$ solution (98 %, Hantech PMC), with air bubbling at a rate of 2 L min^{-1} and a current density of 2.5 A/cm^2. Subsequently, Ti seed layer was etched by Ti etchant (TFT, Transene Company, Inc.) for 10 s. After etching and cleaning with deionized water, Sn was selectively electroless plated onto the Cu using a $SnSO_4$ solution (95 %, CNC tech) in a 1 L bath at 50 ℃ for 15 min.

2.4. Finite element method (FEM) simulation

To replicate the mechanical behavior under shear loading, we used the finite element analysis tool COMSOL Multiphysics. The Solid Mechanics module was used to calculate the shear strength of the structures for various material schemes, such as the nonconductive adhesive layer

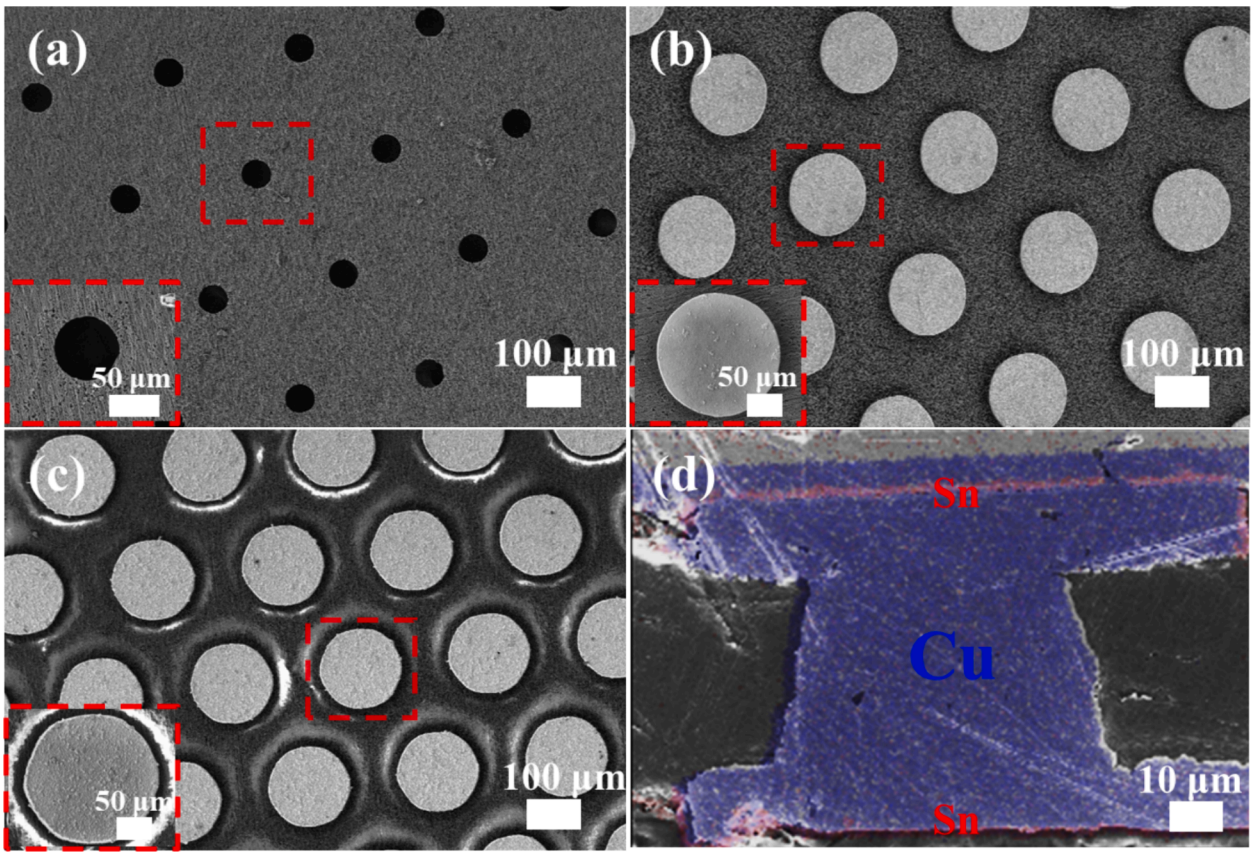


Fig. 2. SEM images of (a) bare PI film with holes, (b) electroplated Cu, and (c) electroless-plated Sn layer. (d) Cross-sectional SEM image with EDS mapping of Sn-coated Cu vias bonded to Sn/Cu pad of testing chips.

(NCA) and NCA/Sn bumps. The order and sizes of all the material layers were comparable to those of the actual test samples. The Young's modulus and Poisson's ratios for Sn, Cu, PI, Al_2O_3, and NCA were assigned as 41 GPa and 0.325; 130 GPa and 0.34; 2.5 GPa and 0.34; 400 GPa and 0.22; and 3.8 GPa and 0.38, respectively. Axial displacement was applied along one edge of the structure, whereas the bottom of the structure was fully constrained to mimic the shear strength test. Physics-based meshing was employed to ensure convergence of the solution using a fine mesh near the interfaces of the material layers.

3. Results and discussion

Fig. 1 shows a schematic of the fabrication process of the holey PI-based flexible interconnection system. PI films with uniformly distributed holes with a diameter of approximately 50 μm were prepared. Ti with a thickness of 50 nm was deposited on one side of the PI film via sputtering as a seed layer for electroplating. Subsequently, the holes were filled with via electroplating, where the diameter of both ends of the Cu via was varied to 100, 140, 160, and 180 μm, depending on the electroplating times (Supporting Fig. 1). Following the Cu electroplating, the Ti seed layer was removed via chemical etching. The fabricated Cu pillars were flipped and electroplated on the back side to create the same structure on the top and bottom sides of the PI film. Next, Sn layers with approximately 500 nm thickness were formed via electroless plating on the PI films (Fig. 1c). As bonding with Cu pillars requires significantly high temperature (>400 ℃) or pressure (>100 MPa), which can result in the warpage of the circuit board and failure of other components in electronic devices [34,35], low-temperature bonding is required for the polymeric substrate in flexible electronic devices. Among the possible options, solder based on Sn, which has a low melting point (231.9 ℃) and good bonding strength, is highly favored. EDS analysis of the head part of the electroplated PI film showed significant signals from Cu (blue) and Sn (red), thereby confirming the successful electroplating of the Cu pillars and Sn bumps on the PI film (Supporting Fig. 2). Additionally, approximately 5 μm of NCA layer was coated outside the bump area. The NCA layer in the empty area, other than the bump, provided a more stable bonding strength. This system using NCA and PI films can completely prevent short-circuit problems that may occur in ACF.

The surface morphology at each fabrication step was examined using SEM and EDS, as shown in Fig. 2. The hole size in PI was approximately 50 μm (Fig. 2a). No significant variation was observed in the sizes of the heads of the electroplated Cu vias (Fig. 2b) and Sn-coated Cu vias (Fig. 2c). Cross-sectional SEM images of the Cu vias showed no significant defects, indicating the excellent quality of the Cu vias (Fig. 2d).

The shear strength of the PI film interconnections was evaluated using a shear stress test instrument (Fig. 3a). The testing chips with Sn/Cu pads were bonded with the holey PI-based flexible interconnection system at a temperature range of 240–270 °C. Fig. 3b shows that the sample was fixed using both holders, and a force was applied at a rate of 100 μm/s by using a 2 mm tip. Tests conducted on samples with varying bump sizes revealed that the total load values increased significantly for larger bump sizes. However, the shear strength values, which were divided by the bonded area, exhibited no significant variation depending on the bump size, as shown in Fig. 3c. The shear strength was more significantly influenced by the bonding temperature; a higher bonding temperature resulted in increased bonding strength (Fig. 3c). Overall, the PI film interconnection system exhibited superior shear strength of 63.76 MPa, thereby significantly surpassing the typical shear strength of 30–40 MPa exhibited by commercially available ACF [28,36–39].

The temperature-dependent differences in the bonding strengths were attributed to the microstructural bonding conditions. Fig. 4 shows

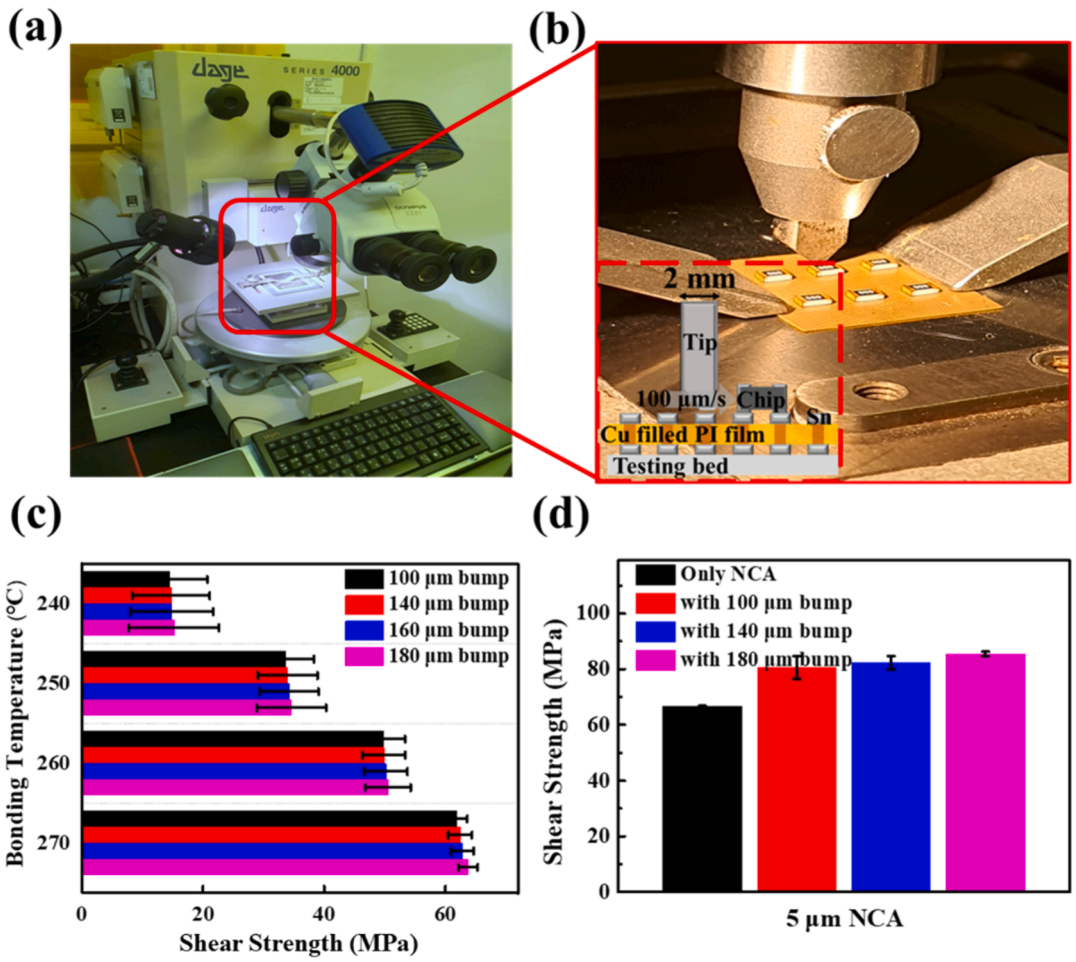


Fig. 3. (a) Photograph of shear bonding test system and (b) enlarged photograph and schematic of (a) red rectangular area. (c) Shear bonding strengths of the samples bonded at different temperature. (d) Shear bonding strengths of PI film interconnection system with NCA according to the bump size.

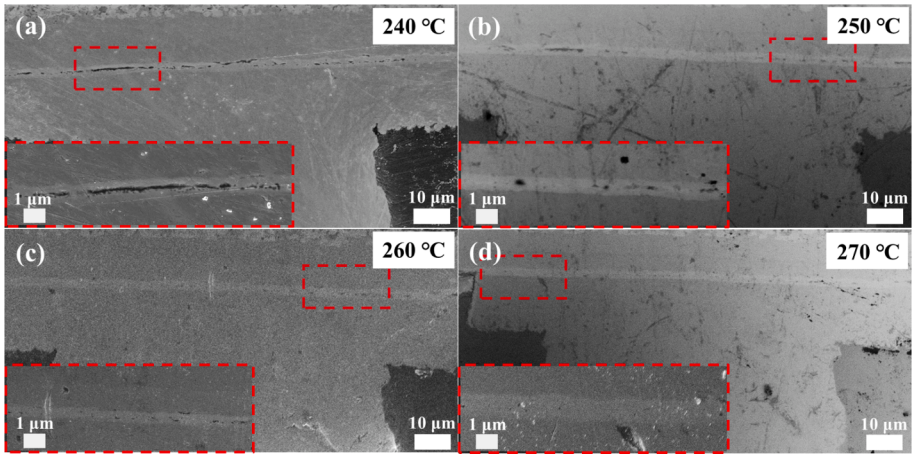


Fig. 4. Cross-sectional SEM images of Cu/Sn/Cu bonded with NCA layer according to (a) 240, (b) 250, (c) 260, and (d) 270 ℃.

the SEM images of the cross-sectional area of the bonded layer of Sn layer and Sn/Cu pad of testing chips at the different bonding temperatures of 240–270 °C. At 240 °C, slightly above the melting point of Sn (231.9 °C), partial bonding was observed, as shown in the enlarged image in Fig. 4a, where a large area still remained unbonded. Even at higher temperatures of 250 and 260 °C (Fig. 4b and c), areas with incomplete bonding were still present (Supporting Fig. 3). Raising the bonding temperature to 270 °C achieved the complete bonding interface (Fig. 4d) without observable defects. The defects or unbonded areas at the interfaces acted as sites for stress concentration that accelerates crack initiation or propagation at a stress level lower than the intrinsic strength of Sn. Therefore, the lower shear bonding strengths of the samples bonded below 270 °C, as observed in Fig. 3c, were because of the limited bonding formation at the interface between Sn layer of PI films and Sn/Cu pads of testing chips. There is a possibility of uneven heat distribution across the entire bonding area, where insufficient heat

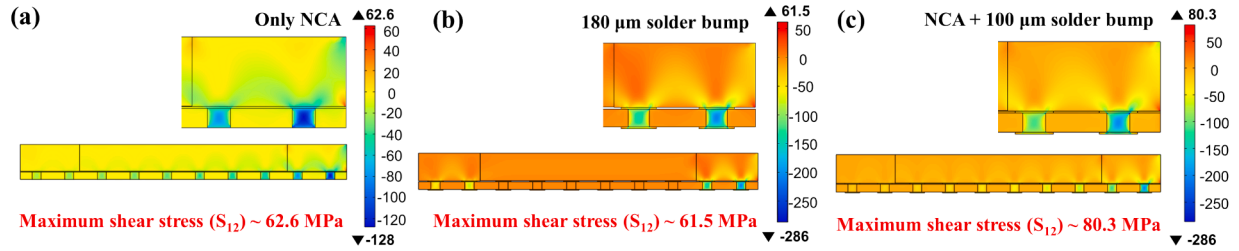


Fig. 5. Damage-equivalent strain distribution illustration of FEM simulation for (a) NCA, (b) Cu-Sn solder bump arrays and (c) NCA+Cu-Sn solder bump arrays.

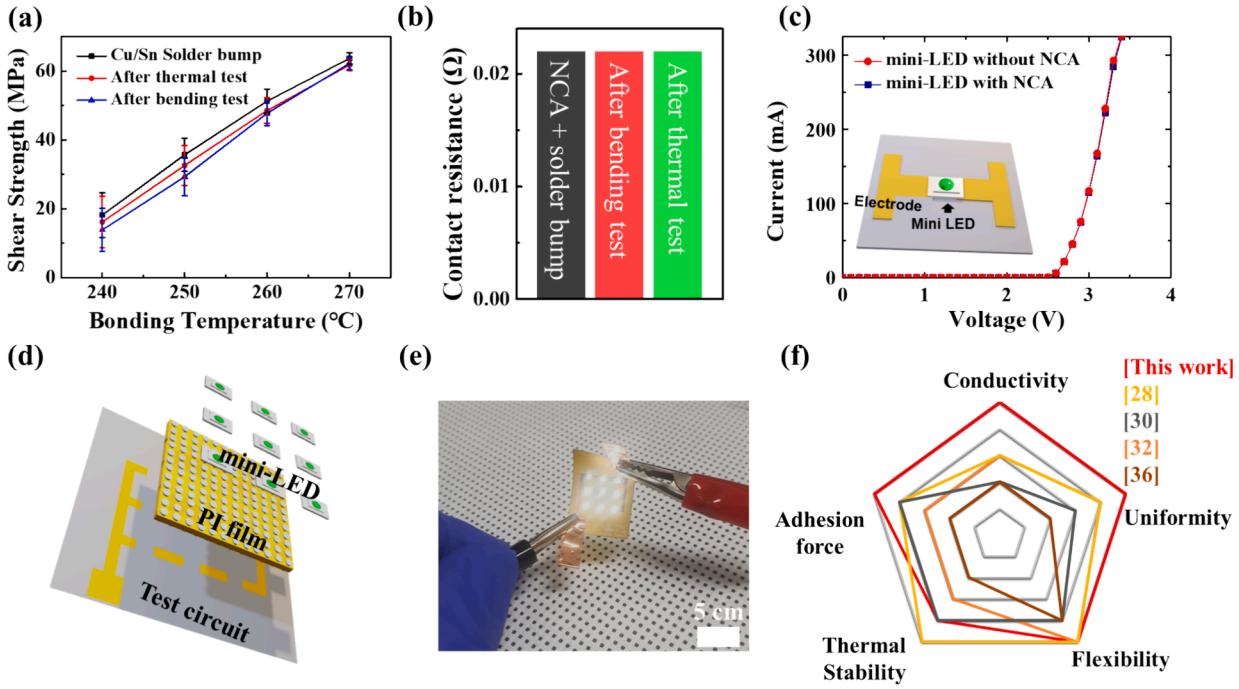


Fig. 6. (a) Shear bonding strength and (b) electrical resistance of testing chips bonded with NCA-coated flexible PI interconnection system after the bending tests of 1,000 cycles (blue line) and ambient durability tests by exposing at 85 ℃, 85 % for 100 h. (c) I–V characteristics of a mini-LED bonded with NCA-coated flexible PI interconnection system. Inset of (c) shows the schematic of I–V characteristics. (d) Schematic of 3*3 array on mini-LEDs bonding and (e) photo of the operation of mini-LED array. (f) Spiderweb chart related with our interconnection system.

may be applied to some portions, resulting in voids. This issue can be resolved by using a higher temperature, which can apply sufficient heat energy across the entire bonding area. Additionally, the higher temperature can accelerate the diffusion of Sn and Cu atoms, promoting the formation of a more perfect interface. Therefore, the higher temperature results in a better interface quality, leading to higher shear strength. According to the equation, $\tau = F/A$, where τ is the shear strength, F is the total load under shear deformation, and A is the bonding area, the shear strength is normalized by the total load and bonding area. Thus, changes in the bonding area at the same bonding temperature showed negligible effects on the shear strength values (Fig. 3c).

Our PI-based flexible interconnection system facilitated bonding with components through soldering of the Sn layer of Cu vias with the metal pads of the testing chips. Thus, there is a vacant area between the holes of the PIs that has no bonding medium for the Sn bump, which does not contribute to bonding. Therefore, we explored the concept of filling the vacant area with NCA to enhance the shear bonding strength of the PI-based flexible interconnection system. Fig. 3d shows the shear bonding strength of the PI-based flexible interconnection system with the NCA layer. The test chips were bonded at 270 °C. The application of NCA significantly enhanced the shear bonding strength, as shown in Fig. 3d. The NCA-coated flexible PI film interconnection system exhibited a shear bonding strength of approximately 85.55 MPa, which was approximately 34 % higher than that of the flexible PI film interconnection system without the NCA. Interestingly, the shear bonding strength of the flexible PI films interconnected with the NCA coating was similar to that of the flexible PI film interconnection system with only Sn/Cu bumps. This indicates that the adhesion of NCA and Sn–Sn soldering resulted in similar adhesion strength values for the bonding of the metal pads and substrates. However, the integration of NCA with Sn–Sn soldering resulted in a synergetic effect on the bonding properties, thus increasing the bonding strength by approximately 34 %. To confirm this synergy, we conducted an FEM simulation using the COMSOL software. At the same strain level, the flexible PI film interconnection system with only NCA or Cu-Sn solder bumps exhibited similar shear stress values (Fig. 5(a–b)). Whereas, the NCA+Cu-Sn solder bumps exhibited higher shear stress values than those of the NCA or Cu-Sn solder bumps (Fig. 5 (c)), which is similar to the experimental results. A mixture of NCA and Cu-Sn soldering provides additional points for heterointerfaces formed by both NCA and Sn/Cu bumps, thereby enhancing the ability to resist the shear force that increases the shear strength.

Fig. 6a and b show the change in shear bonding strength before and after reliability tests, respectively, including bending test with 1.5 mm of bending radius for 1000 cycles and ambient stability tests at 85 ℃, 85 % for 100 h. The shear bonding strength (Fig. 6a) and electrical resistance (Fig. 6b) exhibited no significant change before (63.76 MPa and 22 mΩ)

and after (63.02 MPa and 22 mΩ) the reliability tests. This confirmed the high stability of our flexible PI films interconnection system. We examined the potential of the films as interconnection systems for bonding mini-LEDs. Fig. 6c shows the I–V curves measured for a mini-LED bonded to a flexible PI interconnection system. At a driving voltage of 2.5 V, a sharp increase in the current value was observed, confirming the good operation of the mini-LEDs in our flexible PI interconnection system. We also demonstrate the operation of an array of mini-LEDs, as shown in Fig. 6d. A 3 × 3 array of mini-LEDs was connected to the flexible printed circuit board (FPCB) using the flexible PI interconnection system. As shown in Fig. 6e, the LED array operated successfully, and no change in brightness was observed under manual bending. Successful mini-LED driving tests using the proposed interconnection system represent a potential contribution to the development of next-generation flexible electronic devices.

4. Conclusions

This study successfully demonstrated a flexible interconnection system using a flexible holey PI film filled with a Cu via and Sn solder bumps for bonding electronic chips to flexible substrates. By forming periodic Sn-covered Cu vias through the vertical holes of the PI film, high electrical conductivity and bonding strength for integration with electronic chips were simultaneously achieved. This packaging system with uniformly distributed Sn/Cu vias is free from short-circuit issues, which is the most challenging issue in conventional ACFs. The bonding strength was further improved by adopting an NCA layer, wherein the adhesive/solid bump interfaces bore a larger load than those of a single component. Thermal and mechanical stability tests revealed that our flexible PI-based interconnection system was highly reliable under thermal shock or cyclic bending conditions. In addition, mini-LEDs integrated with an FPCB using our flexible PI-based interconnection system were successfully operated without losing their initial brightness even under deformable conditions. This novel concept of a flexible interconnection system with excellent mechanical, electrical, and thermal properties will contribute significantly to the development of next-generation flexible electronic devices.

CRediT authorship contribution statement

Heebo Ha: Writing – review & editing, Writing – original draft, Visualization, Validation, Methodology, Investigation, Formal analysis, Data curation, Conceptualization. **Byunghoon Lee:** Writing – original draft, Methodology, Investigation, Formal analysis, Conceptualization. **Sooyong Choi:** Writing – review & editing, Writing – original draft, Resources, Methodology, Investigation, Formal analysis, Data curation. **Nadeem Qaiser:** Software, Methodology, Investigation, Formal analysis. **Sera Kwon:** Writing – original draft, Investigation, Formal analysis, Data curation. **Zungsun Choi:** Writing – original draft, Methodology, Investigation. **Chih-Ming Chen:** Writing – original draft, Supervision, Investigation, Data curation. **Byungil Hwang:** Writing – review & editing, Writing – original draft, Supervision, Project administration, Methodology, Investigation, Funding acquisition, Data curation, Conceptualization.

Declaration of competing interest

The authors declare that they have no known competing financial interests or personal relationships that could have appeared to influence the work reported in this paper.

Acknowledgements

Funding: This work was supported by the National Research Foundation of Korea(NRF) grant funded by the Korea government(MSIT) (Nos. RS-2023-00257595, RS-2024-00413272 and 2022K1A3A1A18080009)

Appendix A. Supplementary material

Supplementary data to this article can be found online at https://doi.org/10.1016/j.asej.2024.103064.

References

[1] Keum K, Kim JW, Hong SY, Son JG, Lee SS, Ha JS. Flexible/stretchable supercapacitors with novel functionality for wearable electronics. Adv Mater 2020; 32:2002180.
[2] Choi C, Qaiser N, Hwang B. Mechanically pressed polymer-matrix composites with 3d structured filler networks for electromagnetic interference shielding application. Facta Universitatis, Series. Mech Eng 2023. https://doi.org/10.22190/FUME240601038C. online first.
[3] Hao H, Hui D, Lau D. Material advancement in technological development for the 5G wireless communications. Nanotechnol Rev 2020;9:683–99.
[4] Kim H, Qaiser N, Hwang B. Electro-mechanical response of stretchable pdms composites with a hybrid filler system, Facta Universitatis, Series. Mech Eng 2023; 21:051–61.
[5] Hwang B, Han Y, Matteini P. Bending fatigue behavior of Ag nanowire/Cu thin-film hybrid interconnects for wearable electronics, Facta Universitatis, Series. Mech Eng 2022;20:553–60.
[6] Hu L, Chee PL, Sugiarto S, Yu Y, Shi C, Yan R, et al. Hydrogel-based flexible electronics. Adv Mater 2023;35:2205326.
[7] Ha H, Müller S, Baumann R-P, Hwang B. Peakforce quantitative nanomechanical mapping for surface energy characterization on the nanoscale: A mini-review, Facta Universitatis, Series. Mech Eng 2024;22:1–12.
[8] Milić P, Marinković D, Ćojbašić Ž. Geometrically nonlinear analysis of piezoelectric active laminated shells by means of isogeometric Fe formulation, Facta Universitatis. Series: Mechanical Engineering; 2023. https://doi.org/10.22190/FUME050123059M.
[9] Koo JH, Kim DC, Shim HJ, Kim TH, Kim DH. Flexible and Stretchable Smart Display: Materials, Fabrication, Device Design, and System Integration. Adv Funct Mater 2018;28.
[10] Corzo D, Tostado-Blázquez G, Baran D. Flexible Electronics: Status, Challenges and Opportunities. Frontiers in Electronics 2020;1:594003.
[11] Gao W, Ota H, Kiriya D, Takei K, Javey A. Flexible Electronics toward Wearable Sensing. Acc Chem Res 2019;52:523–33.
[12] Milić P, Marinković D, Klinge S, Ćojbašić Ž. Reissner-mindlin based isogeometric finite element formulation for piezoelectric active laminated shells. Tehnički Vjesnik 2023;30:416–25.
[13] Ha H, Qaiser N, Yun TG, Cheong JY, Lim S, Hwang B. Sensing mechanism and application of mechanical strain sensor: a mini-review, Facta Universitatis, Series. Mech Eng 2023;21:751–72.
[14] Chen Q, Ma Z, Wang Z, Liu L, Zhu M, Lei W, et al. Scalable, robust, low-cost, and highly thermally conductive anisotropic nanocomposite films for safe and efficient thermal management. Adv Funct Mater 2022;32:2110782.
[15] Peng Y, Peng H, Chen Z, Zhang J. Ultrasensitive Soft Sensor from Anisotropic Conductive Biphasic Liquid Metal-Polymer Gels. Adv Mater 2024;36:2305707.
[16] Kim J-H, Lee T-I, Kim T-S, Paik K-W. The effect of anisotropic conductive films adhesion on the bending reliability of chip-in-flex packages for wearable electronics applications. IEEE Transactions on Components: Packaging Manufacturing Technology; 2017. p. 1583–91.
[17] Pal M, Giri A, Kim DW, Shin S, Kong M, Thiyagarajan K, et al. Fabrication of foldable metal interconnections by hybridizing with amorphous carbon ultrathin anisotropic conductive film. ACS Nano 2019;13:7175–84.
[18] Lin Y-S, Xu J-Z, Tien S-W, Hung S-C, Yuan W-L, Chung T-W, et al. Enhanced anisotropic conductive film (ACF) void-free bonding for Chip-On-Glass (COG) packages by means of low temperature plasmas. Microelectron Reliab 2012;52: 2756–62.
[19] Pan Y, Oh S-J, Kim J-H, Kim T-S, Paik K-W. A Study on the Dynamic Bending Property of Chip-on-Flex Assembly Using Anchoring Polymer Layer Anisotropic Conductive Films. IEEE Transactions on Components, Packaging Manufacturing Technology 2020;10:941–8.
[20] Kim S-C, Kim Y-H. Flip chip bonding with anisotropic conductive film [ACF) and nonconductive adhesive (NCA]. Curr Appl Phys 2013;13:S14–25.
[21] Yoon D-J, Malik M-H, Yan P, Paik K-W, Roshanghias A. ACF bonding technology for paper-and PET-based disposable flexible hybrid electronics. J Mater Sci Mater Electron 2021;32:2283–92.
[22] Chang S-M, Jou J-H, Hsieh A, Chen T-H, Chang C-Y, Wang Y-H, et al. Characteristic study of anisotropic-conductive film for chip-on-film packaging. Microelectron Reliab 2001;41.
[23] Palm P, Määttänen J, Tuominen A, Ristolainen E. Reliability of 80 μm pitch flip chip attachment on flex. Microelectron Reliab 2001;41:633–8.
[24] Lau JH. Recent advances and new trends in flip chip technology. J Electron Packag 2016;138:030802.
[25] Rizvi M, Chan Y, Bailey C, Lu H, Sharif A. The effect of curing on the performance of ACF bonded chip-on-flex assemblies after thermal ageing. Soldering Surface Mount Technology 2005;17:40–8.
[26] L. Cao, Z. Lai, J. Liu, Effect of curing condition of adhesion strength and ACA flip-chip contact resistance, Proceedings of the Sixth IEEE CPMT Conference on High

Density Microsystem Design and Packaging and Component Failure Analysis (HDP'04), IEEE, 2004, pp. 254-258.
[27] Uddin M, Alam M, Chan Y, Chan H. Plasma cleaning of the flex substrate for flip-chip bonding with anisotropic conductive adhesive film. J Electron Mater 2003;32:1117–24.
[28] Hwang H, Kong M, Kim K, Park D, Lee S, Park S, et al. Stretchable anisotropic conductive film (S-ACF) for electrical interfacing in high-resolution stretchable circuits. Sci Adv 2021;7:eabh0171.
[29] Lee JS, Kang SJ, Shin JH, Shin YJ, Lee B, Koo JM, et al. Nanoscale-Dewetting-Based Direct Interconnection of Microelectronics for a Deterministic Assembly of Transfer Printing. Adv Mater 2020;32:1908422.
[30] Malik MH, Grosso G, Zangl H, Binder A, Roshanghias A. Flip Chip integration of ultra-thinned dies in low-cost flexible printed electronics; the effects of die thickness, encapsulation and conductive adhesives. Microelectron Reliab 2021;123:114204.
[31] Park J-H, Park JC, Lee S, Paik K-W. Piezoelectric ceramics and flexible printed circuits' interconnection using Sn58Bi solder anisotropic conductive films for flexible ultrasound transducer assembly. IEEE Transactions on Components, Packaging Manufacturing Technology 2019;9:1897–903.
[32] Bo G, Yu H, Ren L, Cheng N, Feng H, Xu X, et al. Gallium–indium–tin liquid metal nanodroplet-based anisotropic conductive adhesives for flexible integrated electronics. ACS Applied Nano Materials 2021;4:550–7.
[33] Hwang B, Qaiser N, Lee C, Matteini P, Yoo SJ, Kim HJJoA. Compounds, Effect of Al2O3/Alucone Nanolayered Composite Overcoating on Reliability of Ag Nanowire Electrodes under Bending Fatigue 2020;846:156420.
[34] Hwang B-U, Jung K-H, Min KD, Lee C-J, Jung S-B. Pressureless Cu–Cu bonding using hybrid Cu–epoxy paste and its reliability. J Mater Sci Mater Electron 2021;32:3054–65.
[35] Panigrahy AK, Chen K-N. Low Temperature Cu–Cu bonding technology in three-dimensional integration: an extensive review. J Electron Packag 2018;140:010801.
[36] Wu G, Tao B, Yin Z. Study on the shear strength degradation of ACA joints induced by different hygrothermal aging conditions. Microelectron Reliab 2013;53:2030–5.
[37] M. Li, J. Tudor, R. Torah, S. Beeby, Stress analysis and optimization of a flip chip on flex electronic packaging method for functional electronic textiles, IEEE Transactions on Components, Packaging Manufacturing Technology, 2017, pp. 186-194.
[38] Ji X, Jin X, Hou C, Xiao G, Fan X, Shu X. Loading rate response on shear mechanical properties of conductive adhesive with different silver contents. Journal of Adhesion Science Technology 2020;34:1935–46.
[39] Nguyen HV, Kristiansen H, Imenes K, Aasmundtveit KE. Peel adhesion and reworkability of anisotropic conductive adhesive for flex-to-flex assembly in medical devices. In: 2020 IEEE 8th electronics system-integration technology conference (ESTC), IEEE; 2020. p. 1-7.



Byungil Hwang is currently an associate professor at the School of Integrative Engineering, Chung-Ang University, Seoul, Republic of Korea. He is working on surface engineering of metal and its application to highly stable electronics packaging system. He is engineering the materials and design to achieve the high quality of materials systems for various applications.